J Appl Biotechnol Rep. 2020 Mar;7(1):41-47

doi 10.30491/JABR.2020.105919

Journal of
Applied Biotechnology Reports

Original Article

The Effect of Protelos Content on the Physicochemical, Mechanical and Biological Properties of Gelatin-Based Scaffolds

Seyyed Behnam Abdollahi Boraei[1], Jhamak Nourmohammadi[1*], Behnaz Bakhshandeh[2], Mohammad Mehdi Dehghan[3,4], Zoilo Gonzalez[5], Begona Ferrari[5]

[1]Department of Life Science Engineering, Faculty of New Sciences and Technologies, University of Tehran, Tehran, Iran
[2]Department of Biotechnology, College of Science, University of Tehran, Tehran, Iran
[3]Department of Surgery and Radiology, Faculty of Veterinary Medicine, University of Tehran, Tehran, Iran
[4]Institute of Biomedical Research, University of Tehran, Tehran, Iran
[5]Instituto de Cerámica y Vidrio, CSIC, c/Kelsen 5, 28049, Madrid, Spain

Corresponding Author: Jhamak Nourmohammadi, PhD, Associate Professor, Department of Life Science Engineering, Faculty of New Sciences and Technologies, University of Tehran, Tehran, Iran. Tel: +98-21-86093264, Email: J_nourmohammadi@ut.ac.ir

Received September 13, 2019; **Accepted** November 30, 2019; **Online Published** March 11, 2020

Abstract

Introduction: Protelos (Pr) is a drug treatment for osteoporosis which reduces the risk of broken bones. The drug is unusual in that it both increases the deposition of new bone by osteoblasts and reduces the resorption of bone by osteoclasts. In this study, the effect of different amounts of Pr on the properties of gelatin-based scaffolds has been investigated.

Materials and Methods: Halloysite nanotube (HNT) was used to control the release of Pr, while the HNT: Pr ratios changed. (2:1 (0.5-GHPr) and 1: 2 (2-GHPr)). For characterization of the scaffolds, the morphology, structure, mechanical behavior, and release behavior of this nanocomposite scaffold were studied. Also, cellular studies such as 3-[4,5-dimethylthiazole-2-yl]-2,5-diphenyltetrazolium bromide (MTT) assay, alkaline phosphatase (ALP) and calcium deposition of the nanocomposite scaffolds were investigated.

Results: As a result, it can be stated that the 2-GHPr nanocomposite scaffold showed the best osteogenesis and release behavior between prepared scaffolds. In the case of mechanical properties, also 2-GHPr scaffolds had the best mechanical strength and modulus.

Conclusions: According to the results, it can be mentioned that 2-GHPr composite scaffolds are a good choice in bone tissue engineering (TE).

Keywords: Protelos, Stem Cell, Halloysite Nanotube, Osteogenesis

Citation: Abdollahi Boraei SB, Nourmohammadi J, Bakhshandeh B, Dehghan MM, Gonzalez Z, Ferrari B. The effect of protelos content on the physicochemical, mechanical and biological properties of gelatin-based scaffolds. J Appl Biotechnol Rep. 2020;7(1):41-47. doi:10.30491/JABR.2020.105919.

Introduction

Nowadays there are a lot of bone defect types which have been caused by infection, deformity, trauma, tumor resection and osteoporosis. This issue is mounting year by year, but there are not enough resources for autogenous and allograft bone graft which makes it extremely difficult to treat all of the patients. Recently, tissue engineering (TE) has appeared to expand viable substitutes capable of reconstructing the structure of bone tissues and to regenerate the functions of damaged bones.[1] The use of porous materials as carriers for the delivery of molecules such as drugs has received remarkable attention due to their structural stability and controllable surface reactivity.[2] These properties provide porous materials such as scaffolds with useful features for loading, encapsulation, and controlled release of drugs, biomolecules, proteins etc.[3,4]

Scaffolds also are being used for cell differentiation, proliferation and spreading to create new tissue.[5] Gelatin scaffolds are widely used in TE because of their low antigenicity, biodegradability, good cell attachment and ability to deliver cells and growth factors.[6] But gelatin does not have good mechanical properties. Halloysite nanotube (HNT) incorporation can improve the mechanical properties of the polymers due to being tough and also their high aspect ratio.[7] At the first, Halloysite ($Al_2Si_2O_5(OH)_4 \cdot nH_2O$) was characterized by Berthier (1826) as a dioctahedral 1:1 clay mineral of the kaolin group[8] which has a mainly hollow tubular structure in the submicron range and is chemically similar to kaolin.[9] It originates naturally and can be extracted as a raw mineral from the mine which makes it economically cost-effective. Neighboring alumina and silica layers, and their waters of hydration create packing disarray which lead to the layers to curve into tubes.[10] Normally, HNTs have a 15 nm lumen with 30-50 nm external diameter and a length of nearly 1 micron.[11] Actually, HNTs are specific materials

with a unique combination of the tubular nanostructure, large aspect ratio, natural availability, rich functionality, good biocompatibility, and high mechanical strength. These features generate unusual mechanical, thermal and biological properties.[7] The HNT has also some other advantages, such as hydrophilicity, good dispersion capacity, and loading drugs ability.[12] Due to its non-toxic property, HNTs can be used for cell-mediated assembly and for the capture of around free cells.[13] As a kind of natural inorganic nanofillers, HNTs have been added into the polymer matrix as an environmentally benign reinforcing material, which can significantly enhance mechanical properties, serve as nucleating agent, increase thermal stability and flame retardancy.[14] In some studies, HNTs were used to encapsulate a model drug first, and then the drug-loaded HNTs were mixed with biocompatible polymer (natural or synthetic) solution for forming composite drug-loaded scaffolds.[15] Protelos (Pr) is a divalent strontium salt of ranelic acid which is used as a treatment of bone problems and can load onto HNTs. Pr has a dual role: bone-forming and bone-resorbing which improves bone microarchitecture.[16] This effect of Pr has been reported in several animal studies that correspond with in vitro studies.[17]

The aim of this study was to evaluate the effect Pr amounts on the osteogenesis behavior of 3D gelatin-based scaffolds which are produced by the freeze-drying technique. The morphological and structural properties of the prepared scaffolds were characterized. Also, the drug release and cellular behavior of the scaffolds were investigated.

Materials and Methods

Gelatin was purchased from the Tetrachem Company. The HNT was provided by Sigma Aldrich Company, USA. The Pr was purchased from Servier Company, France. Also, High Glucose Dulbecco's Modified Eagle's Medium (DMEM-HG), phosphate buffered saline (PBS), penicillin-streptomycin, and fetal bovine serum (FBS) were bought from GIBCO Company, Ireland. Isolation, expansion and characterization of rat mesenchymal stem cell (MSC) were performed as described previously.[18,19]

Preparation of Gelatin-Based Scaffolds

Freeze-drying was carried out with an FDB-5503 dryer (OPERON company, Korea). At first, gelatin was dissolved in dH_2O with a concentration of 6 wt. % at 40 °C. The HNT was added and dispersed by stirring in the gelatin solution for 24 hours. Then the gelatin solutions with HNT (GH) were then stored at -20 and -80°C in the freezers, respectively, and later placed in the freeze-drier cooling up to -50°C for 72 hours.

In order to load Pr on HNT, the Pr: HNT ratios (0.5 and 2) were mixed together in dH_2O and stirred overnight. The prepared suspension was centrifuged and cleaned with dH_2O twice and the supernatant was poured out. The remaining solid powder was placed in an oven at 30°C for 24 hours. Then, the drug-loaded Halloysite powder was added to the gelatin solution (6 wt. %) and dispersed by stirring. Finally, the suspension was stored in -20 freezer and -80°C freezers, respectively, and samples were placed in freeze-drier at -50°C for 72 hours.

The prepared scaffolds made on GH and GHPr were immersed in glutaraldehyde for 3 hours for the crosslinked treatment and were then washed with 0.01 wt. % of glycine solution for 30 minutes and PBS for 5 minutes. This process was repeated twice.

Characterization of Fabricated Scaffolds

The morphology of the scaffolds was characterized by field emission scanning electron microscopy (FE-SEM; S-4700 model, HITACHI Company). The dispersion of the Pr-loaded HNTs into the gelatin-based scaffolds was inspected by energy dispersive spectroscopy (EDS) elemental mapping in FE-SEM.

The crystallography of the scaffolds was studied by X-ray diffraction (XRD) in a D8 ADVANCE diffractometer (BRUKER Company, UK) with Cu-K_α radiation, voltage of 40 kV and speed of 2°/min, while the crosslinked structure of the GH and GHPr scaffolds were evaluated by Fourier-transform infrared (FTIR) spectroscopy (Spectrum 100 model, PerkinElmer Company, UK) over a range of 4000–400 cm^{-1}.

The compressive behavior of the scaffolds (GH, 0.5-GHPr and 2-GHPr) was determined by the ZWICK/ROEL Z005 testing machine (ZWICK, Germany). Samples were specifically shaped and/or machined for compressive tests down to 10 mm in diameter and 10 mm in height. The cross-head speed was 1 mm/min.

In Vitro Release Study of Protelos From the Scaffolds

In order to characterize the Pr release behavior, the scaffolds were incubated in PBS at 37°C on a 90 rpm/min shaker incubator. A UV-Visible instrument (NANODROP 2000c, Thermo Scientific Company, USA) was employed to determine the amount of released drug until 21 days at the wavelength of 318 nm.

Cellular Assay

The MSCs were extracted from the tibia of the rat; then they were cultured in DMEM complete media. The media included 20% FBS and 1% antibiotics/antimycotics (final concentration: penicillin 100 units/mL, streptomycin 100 mg). All cellular experiments were done by the second-passage of cells.

MTT Assay

The MTT assay was employed to measure the cytotoxicity of the samples. Porous scaffolds were placed in 48-well culture plate and MSCs were seeded (20 000 cells/well) on them. Then they were cultured in DMEM (15% FBS) at 5% CO_2 and 37°C in the incubator for 1, 4 and 7 days. After time culture, 30 µL MTT was added into each well, and incubation proceeded for 3 hours. Then, 200 µL DMSO was added to cells and were kept for 30 minutes in a dark place. Finally, the absorption amount was measured at a wavelength of 570 nm using an ELISA plate reader.

Alkaline Phosphatase Activity

Alkaline phosphatase (ALP) activity assessment was evaluated by using 200 µL of RIPA buffer. The total protein

was extracted from stem cells cultured on TCPS and different coatings after 7 and 14 days. For sedimentation of cell debris, the lysate was centrifuged at 1200 rpm at 4°C for 5 minutes. Finally, the supernatant was collected and ALP activity was measured with an ALP assay kit (Parsazmun, Tehran, Iran).

Calcium Deposition

Alizarin red staining method was used to measure the amount of calcium deposited on the 3D-scaffolds; simultaneously with osteogenesis differentiation of MSCs. At first, the prepared samples were sterilized with irradiation of UV light for 20 minutes for each side of the scaffolds. The procedure followed by rinsing with PBS for 3 times; then the scaffolds were immersed in cell culture medium for 7 and 14 days in a humidified incubator at 37°C with 5% CO_2. The culture medium contained high glucose DMEM and osteogenic factors (10 mM Beta-Glycerophosphate, 50×10^{-6} g/mL L-ascorbic acid and 10^{-7} mM dexamethasone) The medium was changed every three days. At the end of each time point, cell–scaffold constructs were used for Ca assay. After 7 and 14 days of incubation, cell-scaffold constructs were fixed by 2.5% Glutaraldehyde at 4°C for 1 hour and subsequently were placed in 50, 70, 80 (for 15 minutes), 96 and 100% (for 7-10 minutes) ethanol, respectively. Then Alizarin red-40 mM was added to the scaffold for 20-30 minutes. Phase microscopy was employed to observe the calcium deposited areas. In order to quantify the calcium deposited amount, the red matrix precipitate was solubilized in 10% Acetic acid (Sigma-Aldrich, USA). Finally, optical density was read at 405 nm. Each test was repeated three times.

Statistical Analysis

All experiments were performed at least three times and the obtained data were expressed as the mean ± standard deviation (SD). Differences between the samples were assessed using one-way ANOVA. The results were considered statistically significant at the $P < 0.05$ level.

Results and Discussion

Characterization of the Scaffolds

A suitable scaffold should meet certain criteria, such as providing an interconnected 3D porous structure for cell growth and nutrient transport. In Figure 1, the typical porous structure of freeze-dried samples was observed for the three shaped scaffolds (GH, 0.5-GHPr and 2-GHPr).[20] In all samples, a highly porous and interconnected network structure formed by lattice-like holes was observed by FE-SEM. As expected, GH scaffold exhibited the largest pores with the diameter of 297.21 ± 53.76 µm. However, the pore size decreases to 234.34 ± 36.87 µm in 0.5-GHPr and 118.94 ± 43.80 µm in 2-GHPr scaffold. This reduction might be due to the electrostatic interaction of strontium ions in Pr with negative charges of HNTs.[21] Although Scaffolds with a larger mean size of pores (> 100 µm) can provide suitable matrices for bone regeneration.[22]

Figure 2 shows the microstructure of the wall of the GHPr scaffold at a higher magnification as well as the punctual EDS analysis of the sample. The high dispersion of the HNTs is visible in the scaffold walls. From the EDS analyses, Al and Si elements were considered as main components of the HNTs, while Pr was also detected in the punctual analysis of HNT, indicating the successful loading of Pr on HNTs.

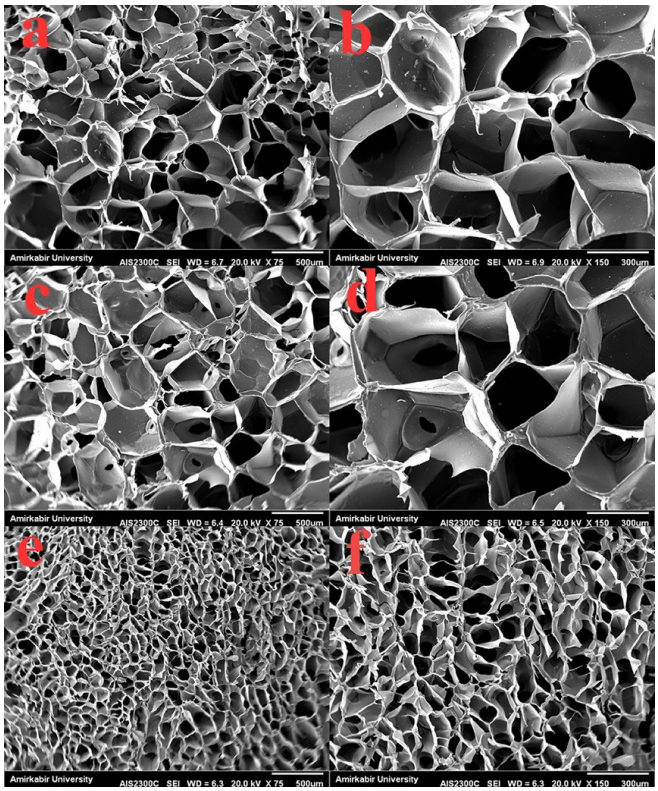

Figure 1. Micrographs of the GH (a and b), 0.5-GHPr (c and d) and 2-GHPr (e and f) Freeze Dried Scaffolds.

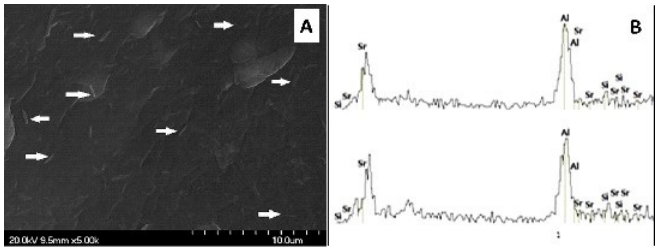

Figure 2. FE-SEM Images and EDS Analyses of the GHPr Scaffold.

Figure 3 shows the XRD patterns of the as-received HNT, 0.5-GHPr and 2-GHPr porous scaffolds, respectively. The pattern of the GH scaffold was typical of partially crystalline gelatin with a broad peak located at 2θ = ~19°. This characteristic peak is usually assigned to the triple-helical crystalline structure of gelatin.[23] In the GH composite, the diffraction peaks of the freeze-dried structure are in accordance with the combination of HNT and Gel characteristic peaks. In general, the diffraction profiles of HNT and Gel are weakened in GH samples but, although the relatively low amount of HNT included in the scaffold (<4%), the (001) basal plane peak of HNT is evident in the composite, and it is placed at 2θ = 11.9°. This constitutes the evidence of the inalterability of the HNT crystal structure during the scaffold processing.[24] On

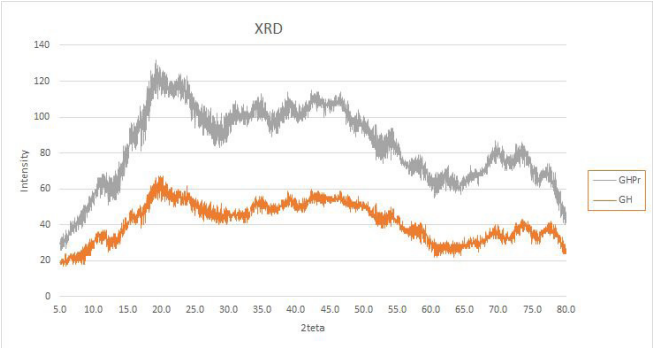

Figure 3. X-Ray Diffraction Pattern of the GH and GHPr Scaffolds.

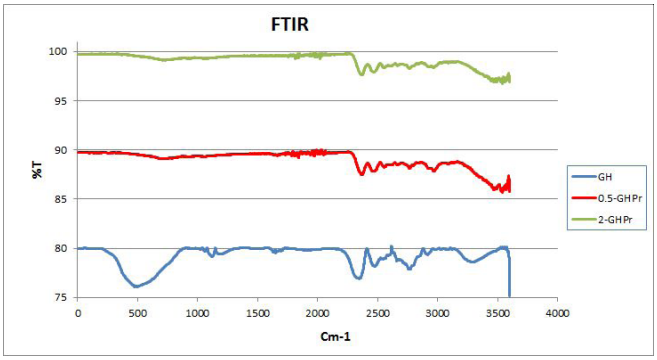

Figure 4. FTIR Spectra of the GH, 0.5-GHPr and 2-GHPr Scaffolds

the other hand, although the Pr diffraction pattern shows characteristic sharp crystalline peaks,[25] none of these peaks were evident for the GHPr scaffolds. The addition of Pr to the GH scaffold causes a small increase in the intensity of the characteristics peaks of the GH pattern and the slight shift of the (001) peak of HNT to 11.2°, which indicates the possible insertion of the strontium in the interlayer spaces of silicate at the Halloysite structure.[25] The crystalline Pr was not detected in the scaffold structure evidencing its dissolution and then adsorption on the cargo. Consequently, the interaction at the molecular level of the Pr and the Halloysite during mixing in the aqueous suspension is demonstrated.

The FTIR analysis was used to determine the chemical interaction of HNT and Pr with the gelatin matrix, which defines the structure of 3D-scaffolds and their biological behavior and drug delivery. Figure 4 shows the FTIR spectra collected for all the 3D scaffolds under study. In a study, the FTIR spectra of gelatin showed the major peaks in three different Amide regions in 1660-1610 cm^{-1} (Amide-I), 1560-1510 cm^{-1} (Amide-II), 1240-450 cm^{-1} (Amide-III) regions.[26] The spectra of composite materials (GH and GHPr) mainly showed the characteristic peaks of gelatin.[27] Also, the Al-OH stretching peaks between 3690 cm^{-1} and 3615 cm^{-1} disappear in the spectrum of the composite material suggesting the reaction between gelatin and halloysite Al–OH groups and the loss of hydrated water. This fact can be also supported when the spectral range between 1100 and 1000 cm^{-1} is inspected. This wavelength range includes the vibrations arising from stretching vibrations of the carbohydrate, ν(C-O) and ν(C-O-C) at 1078 and 1028 cm^{-1} in the Gel scaffold, which slightly shifts to higher wavelengths and intensified when HNT and Pr are added, pointing out to the interaction of carbohydrate groups of the gelatin and the Al-OH exposed groups of Halloysite and Pr.[24] Finally, the intensification of the spectra at lower wavelengths in GH and GHPr scaffolds is due to the characteristic peaks of halloysite placed at 697, 530 and 467 cm^{-1} indicatives of the Si-O stretching Al-O-Si bending and the Al-O stretching vibration.[24]

The compressive test of scaffolds is essential in TE and clinical operations. The compressive yield strength and modulus charts of the scaffolds are shown in Figure 5. It can be seen that after incorporation of the Pr, the compressive yield strength and modulus were increased due to two main reasons: 1) the high loading and reinforcing of Pr onto the

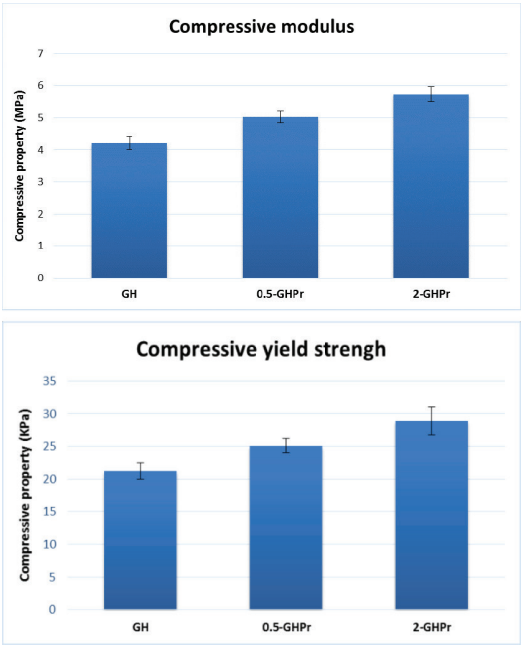

Figure 5. Compressive Properties of the GH, 0.5-GHPr and 2-GHPr Scaffolds.

HNT can be ascribed to the ability of bearing and conveying the force (stress) through the composite interfaces, and 2) due to the demonstrated existence of the physical interaction (hydrogen and electrostatic bonds) between gelatin matrix and HNT. Also, the SEM results showed that after loading of Pr, the pore goes to the lower diameter and higher uniformity that can help to strengthen the scaffolds. It has been reported that decreasing the pore size of the scaffolds enhanced their compressive mechanical strength and modulus.[28] Accordingly, since the 2-GHPr porous scaffold showed good mechanical properties, it has potential applications in bone TE.[29]

In Vitro Pr Release Studies

Data from the Pr release in PBS medium performed on the 3D-scaffold is presented in Figure 6. The loading and releasing goal of this drug carrier (HNT) was to acquire a new drug carrier for Pr and perceive the scheduled time-release behavior. The washing procedure (twice with glycine and twice with PBS) was found to reduce the initial burst release significantly. After 500 hours (21 days), about 37% and 47%

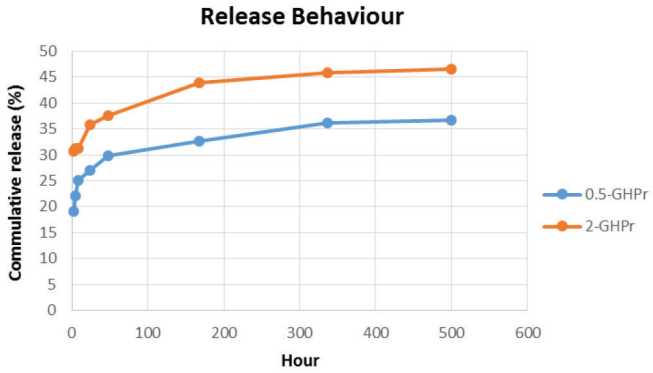

Figure 6. Pr Release Behavior From the Freeze Dried Scaffold in PBS.

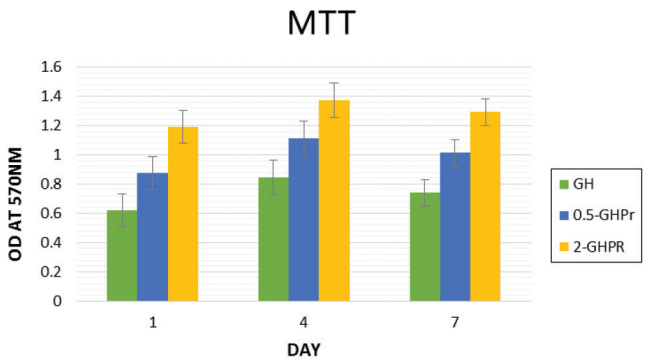

Figure 7. MTT Assay of MSCs Proliferation and Viability on the GH, 0.5-GHPr and 2-GHPr Scaffolds During 1, 4 and 7 Days of Culture.

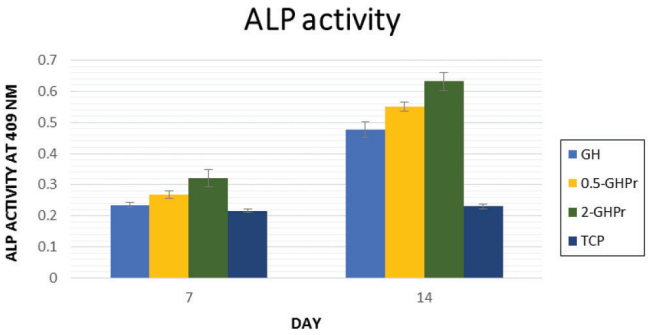

Figure 8. Alkaline Phosphatase (ALP) Activity in MSCs on Samples (GH, 0.5-GHPr and 2-GHPr) and Tissue Culture Polystyrene at 7 and 14 Days, During Osteogenic Differentiation ($P < 0.05$).

of Pr was released from 0.5-GHPr and 2-GHPr, respectively. The increase in the percentage of drug release from a 2-GHPr scaffold can be attributed to the completely hydrophilic nature of the SrR. Since the SrR amount in the 2-GHPr scaffold was higher than 0.5-GHPr, so the rate and amount and percentage of SrR release in the 2-GHPr scaffold was expected. Such sustained release of SrR can be attributed to its interaction with HNTs as confirmed by FTIR and XRD results.

In order to induce proper osteogenic differentiation, Pr has to be released continuously for 21 days.[30] There are several studies that confirmed the HNT ability for sustained release of drugs.[31] The sustained release of Pr can be attributed to the bonding of Pr in the core of HNT or onto the surface of HNT. There are two suggested mechanisms for the release of Pr from HNTs; 1) given the fact that the surface of HNTs due to the presence of Si-O-Si groups has a negative charge, there is the possibility of bonding between positively charged strontium on the surface; 2) Due to the presence of a positive-charge Al $(OH)_2$ (aluminum hydroxide) in the core of HNT, the drug can be bonded from the ranelate negative terminal.

Cellular Studies

Good TE scaffold should be biocompatible and nontoxic. To evaluate the cytocompatibility of the 3D-scaffolds, the MSCs were cultured on the prepared scaffolds, and MTT assay was done (Figure 7). It was found that the proliferation of cells on 2-GHPr scaffolds after days 1, 4 and 7 was better than the GH and 0.5-GHPr samples. Cell growth rate and living cells were found to be reduced a little for all samples; due to forming a complete and homogenous layer of MSCs after day 7, which caused intercellular contact inhibition.[32] All of the GH and GHPr scaffolds gave a significant cell-viability, upon incubation with the extract obtained at 1, 4 and 7 days.[33]

ALP activity assay was done to evaluate the osteogenic ability of MSCs. This enzyme is well-known as one of the earliest osteogenic markers. Several studies have proven that ALP has a relevant key role in osteogenic differentiation since it enhances the mineralization of calcium phosphate cement, the final osteogenic differentiation marker of stem cells.[34] Figure 8 shows a comparison study that applied to all scaffolds for 14 days. The results show an increasing trend during the ALP assay study, proving that scaffolds containing Pr displayed better osteogenic behaviour after 7 and 14 days. Moreover, the ALP activity is highest in cultures grown on the 2-GHPr scaffold. That is, considering that the content of released Pr is larger in 2-GHPr, which improves cell differentiation. Finally, it can be stated that although the Pr delivery does not significantly affect the MSCs growth after the first week of immersion, as it was shown in Figure 7, improvements in osteogenic differentiation were clearly observed in cultures on Pr-scaffolds after 14 days, with respect to the GH scaffold.

Calcium deposits are found in the body, particularly in bone tissues. To confirm the matrix mineralization and differentiation of 3D-scaffolds, an alizarin red staining was performed on the samples for 7 and 14 days of culture.[35] As shown in Figure 9, the calcium content increased after 14 days of differentiation. Also, 2-GHPr scaffold exhibited the highest increment among all the samples. The calcium depositions in Pr-scaffolds was higher than the depositions in pure GH scaffold.[36] Therefore, it can be inferred that the GHPr scaffolds promoted the osteogenic differentiation of MSCs. The osteogenic induction potential of Pr has been reported previously and several mechanisms have been extracted and proposed.[37] Zheng et al[38] have proved that strontium can interact with the mitogen-activated protein kinase signaling pathway and then improve the osteogenic differentiation. Also, Caverzasio and Thouverey[39] have shown that strontium could enhance osteoblast synthetic activity by interacting with the fibroblast growth factor receptors.

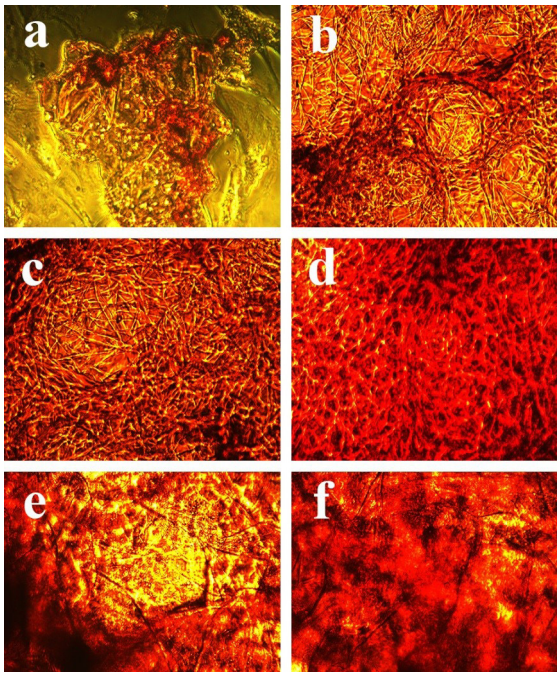

Figure 9. Qualification of the Mineralized GH (a and b), 0.5-GHPr (c and d) and 2-GHPr (e and f) Scaffolds Stained with Alizarin red. Cells were cultured under mineralizing conditions for 7 and 14 days.

Conclusions

In this study, the 3D interconnected porous structures with pore sizes of about 300 microns were produced. The addition of Pr in the GH matrix exhibits a significant change in the morphological and structural properties of the scaffolds. About 37% and 47% cumulative release of Pr was achieved after a sustained release of 500 hours. The sustained release of Pr can be seen till 21 days, due to Pr loading in/onto of HNT. There was no toxic sign after adding Pr to the GH scaffold. The cellular studies were done as the culture on MSCs proved that ALP activity and calcium significantly increased in 2-GHPr scaffold compared to the other scaffolds. To conclude, the 2-GHPr scaffold in this study provided a good porous 3D-structure for bone TE.

Authors' Contributions

All authors equally contributed to the current study.

Conflict of Interest Disclosures

The authors declare they have no conflicts of interest.

Funding/Support

This work was partially funded by University of Tehran for PhD grant [No. 30109/06/16], Institute of ceramic and glass ((ICV-CSIC), Madrid, Spain), and the Community of Madrid (S2017/BMD-3867 RENIMCM) and co-financed with Structural Funds of the European Union and Comunidad de Madrid (ADITIMAT: S2018/NMT-4411, and MERA.NET PCIN-2017-036 (MINECO, Spain). The CNIC was funded by the Ministry of Science, Innovation and Universities and the Pro CNIC Foundation, and was a Severo Ochoa Center of Excellence (SEV-2015-0505).

Acknowledgments

The authors would like to thank the University of Tehran, Iran and the Institute of Ceramic and Glass, CSIC, Madrid, Spain for all their support and technical assistance.

References

1. Langer R, Vacanti JP. Tissue engineering. Science. 1993;260(5110):920-926. doi:10.1126/science.8493529.
2. Martucci A, Pasti L, Marchetti N, Cavazzini A, Dondi F, Alberti A. Adsorption of pharmaceuticals from aqueous solutions on synthetic zeolites. Microporous Mesoporous Mater. 2012;148(1):174-183. doi:10.1016/j.micromeso.2011.07.009.
3. Mizushima Y, Ikoma T, Tanaka J, et al. Injectable porous hydroxyapatite microparticles as a new carrier for protein and lipophilic drugs. J Control Release. 2006;110(2):260-265. doi:10.1016/j.jconrel.2005.09.051.
4. Horcajada P, Márquez-Alvarez C, Rámila A, Pérez-Pariente J, Vallet-Regí M. Controlled release of Ibuprofen from dealuminated faujasites. Solid State Sci. 2006;8(12):1459-1465. doi:10.1016/j.solidstatesciences.2006.07.016.
5. Zhang H, Chen Z. Fabrication and characterization of electrospun PLGA/MWNTs/hydroxyapatite biocomposite scaffolds for bone tissue engineering. J Bioact Compat Polym. 2010;25(3):241-259. doi:10.1177/0883911509359486.
6. Nöth U, Rackwitz L, Steinert AF, Tuan RS. Cell delivery therapeutics for musculoskeletal regeneration. Adv Drug Deliv Rev. 2010;62(7-8):765-783.doi:10.1016/j.addr.2010.04.004.
7. Du M, Guo B, Jia D. Newly emerging applications of halloysite nanotubes: a review. Polym Int. 2010;59(5):574-582. doi:10.1002/pi.2754.
8. Zhang Y, Tang A, Yang H, Ouyang J. Applications and interfaces of halloysite nanocomposites. Applied Clay Science. 2016;119(Pt 1):8-17. doi:10.1016/j.clay.2015.06.034.
9. Price RR, Gaber BP, Lvov Y. In-vitro release characteristics of tetracycline HCl, khellin and nicotinamide adenine dineculeotide from halloysite; a cylindrical mineral. J Microencapsul. 2001;18(6):713-722. doi:10.1080/02652040010019532.
10. Veerabadran NG, Price RR, Lvov YM. Clay nanotubes for encapsulation and sustained release of drugs. Nano. 2007;2(2):115-120. doi:10.1142/S1793292007000441.
11. Tao D, Higaki Y, Ma W, et al. Chain orientation in poly(glycolic acid)/halloysite nanotube hybrid electrospun fibers. Polymer. 2015;60:284-291. doi:10.1016/j.polymer.2015.01.048.
12. Liu M, Dai L, Shi H, Xiong S, Zhou C. In vitro evaluation of alginate/halloysite nanotube composite scaffolds for tissue engineering. Mater Sci Eng C Mater Biol Appl. 2015;49:700-712. doi:10.1016/j.msec.2015.01.037.
13. Konnova SA, Sharipova IR, Demina TA, et al. Biomimetic cell-mediated three-dimensional assembly of halloysite nanotubes. Chem Commun (Camb). 2013;49(39):4208-4210. doi:10.1039/c2cc38254g.
14. Guo B, Zou Q, Lei Y, Jia D. Structure and performance of polyamide 6/halloysite nanotubes nanocomposites. Polym J. 2009;41(10):835-842. doi:10.1295/polymj.PJ2009110.
15. Qi R, Guo R, Zheng F, Liu H, Yu J, Shi X. Controlled release and antibacterial activity of antibiotic-loaded electrospun halloysite/poly(lactic-co-glycolic acid) composite nanofibers. Colloids Surf B Biointerfaces. 2013;110:148-155. doi:10.1016/j.colsurfb.2013.04.036.
16. Ibrahim MR, Singh S, Merican AM, et al. The effect of strontium ranelate on the healing of a fractured ulna with bone gap in rabbit. BMC Vet Res. 2016;12(1):112. doi:10.1186/s12917-016-0724-6.
17. Hott M, Deloffre P, Tsouderos Y, Marie PJ. S12911-2 reduces bone loss induced by short-term immobilization in rats. Bone. 2003;33(1):115-123. doi:10.1016/s8756-3282(03)00115-7.
18. Parfitt AM, Drezner MK, Glorieux FH, et al. Bone histomorphometry: standardization of nomenclature, symbols, and units. Report of the ASBMR Histomorphometry Nomenclature Committee. J Bone Miner Res. 1987;2(6):595-610. doi:10.1002/jbmr.5650020617.
19. Sadeghi M, Bakhshandeh B, Dehghan MM, Mehrnia MR, Khojasteh A. Functional synergy of anti-mir221 and nanohydroxyapatite scaffold in bone tissue engineering of rat skull. J Mater Sci Mater Med. 2016;27(8):132. doi:10.1007/s10856-016-5746-x.

20. Offeddu GS, Ashworth JC, Cameron RE, Oyen ML. Multi-scale mechanical response of freeze-dried collagen scaffolds for tissue engineering applications. J Mech Behav Biomed Mater. 2015;42:19-25. doi:10.1016/j.jmbbm.2014.10.015.
21. Liao J, Qu Y, Chu B, Zhang X, Qian Z. Biodegradable CSMA/PECA/graphene porous hybrid scaffold for cartilage tissue engineering. Sci Rep. 2015;5:9879. doi:10.1038/srep09879.
22. Ghaee A, Nourmohammadi J, Danesh P. Novel chitosan-sulfonated chitosan-polycaprolactone-calcium phosphate nanocomposite scaffold. Carbohydr Polym. 2017;157:695-703. doi:10.1016/j.carbpol.2016.10.023.
23. Peña C, de la Caba K, Eceiza A, Ruseckaite R, Mondragon I. Enhancing water repellence and mechanical properties of gelatin films by tannin addition. Bioresour Technol. 2010;101(17):6836-6842. doi:10.1016/j.biortech.2010.03.112.
24. White RD, Bavykin DV, Walsh FC. The stability of halloysite nanotubes in acidic and alkaline aqueous suspensions. Nanotechnology. 2012;23(6):065705. doi:10.1088/0957-4484/23/6/065705.
25. Nair BP, Sindhu M, Nair PD. Polycaprolactone-laponite composite scaffold releasing strontium ranelate for bone tissue engineering applications. Colloids Surf B Biointerfaces. 2016;143:423-430. doi:10.1016/j.colsurfb.2016.03.033.
26. Shankar S, Teng X, Li G, Rhim JW. Preparation, characterization, and antimicrobial activity of gelatin/ZnO nanocomposite films. Food Hydrocoll. 2015;45:264-271. doi:10.1016/j.foodhyd.2014.12.001.
27. Cebi N, Durak MZ, Toker OS, Sagdic O, Arici M. An evaluation of Fourier transforms infrared spectroscopy method for the classification and discrimination of bovine, porcine and fish gelatins. Food Chem. 2016;190:1109-1115. doi:10.1016/j.foodchem.2015.06.065.
28. Bignon A, Chouteau J, Chevalier J, et al. Effect of micro- and macroporosity of bone substitutes on their mechanical properties and cellular response. J Mater Sci Mater Med. 2003;14(12):1089-1097. doi:10.1023/b:jmsm.0000004006.90399.b4.
29. Amir Afshar H, Ghaee A. Preparation of aminated chitosan/alginate scaffold containing halloysite nanotubes with improved cell attachment. Carbohydr Polym. 2016;151:1120-1131. doi:10.1016/j.carbpol.2016.06.063.
30. Martins A, Duarte AR, Faria S, Marques AP, Reis RL, Neves NM. Osteogenic induction of hBMSCs by electrospun scaffolds with dexamethasone release functionality. Biomaterials. 2010;31(22):5875-5885. doi:10.1016/j.biomaterials.2010.04.010.
31. Hanif M, Jabbar F, Sharif S, Abbas G, Farooq A, Aziz M. Halloysite nanotubes as a new drug-delivery system: a review. Clay Miner. 2016;51(3):469-477. doi:10.1180/claymin.2016.051.3.03.
32. Kalani MM, Nourmohammadi J, Negahdari B. Osteogenic potential of Rosuvastatin immobilized on silk fibroin nanofibers using argon plasma treatment. Biomed Mater. 2018;14(2):025002. doi:10.1088/1748-605X/aaec26.
33. Zhao Y, Guo D, Hou S, et al. Porous allograft bone scaffolds: doping with strontium. PLoS One. 2013;8(7):e69339. doi:10.1371/journal.pone.0069339.
34. Ardeshirylajimi A, Mossahebi-Mohammadi M, Vakilian S, et al. Comparison of osteogenic differentiation potential of human adult stem cells loaded on bioceramic-coated electrospun poly (L-lactide) nanofibres. Cell Prolif. 2015;48(1):47-58. doi:10.1111/cpr.12156.
35. Kharaziha M, Fathi MH, Edris H, Nourbakhsh N, Talebi A, Salmanizadeh S. PCL-forsterite nanocomposite fibrous membranes for controlled release of dexamethasone. J Mater Sci Mater Med. 2015;26(1):5364. doi:10.1007/s10856-014-5364-4.
36. Su WT, Wu PS, Huang TY. Osteogenic differentiation of stem cells from human exfoliated deciduous teeth on poly(epsilon-caprolactone) nanofibers containing strontium phosphate. Mater Sci Eng C Mater Biol Appl. 2015;46:427-434. doi:10.1016/j.msec.2014.10.076.
37. Pilmane M, Salma-Ancane K, Loca D, Locs J, Berzina-Cimdina L. Strontium and strontium ranelate: Historical review of some of their functions. Mater Sci Eng C Mater Biol Appl. 2017;78:1222-1230. doi:10.1016/j.msec.2017.05.042.
38. Chen Y, Zheng Z, Zhou R, et al. Developing a strontium-releasing graphene oxide-/collagen-based organic-inorganic nanobiocomposite for large bone defect regeneration via MAPK signaling pathway. ACS Appl Mater Interfaces. 2019;11(17):15986-15997. doi:10.1021/acsami.8b22606.
39. Caverzasio J, Thouverey C. Activation of FGF receptors is a new mechanism by which strontium ranelate induces osteoblastic cell growth. Cell Physiol Biochem. 2011;27(3-4):243-250. doi:10.1159/000327950.